

Defect detection in photovoltaic modules using electroluminescence imaging

Amine Mansouri¹, Martin Bucher¹, Frederick Koch¹, Marcus Zettl¹, Omar Stern¹, Mark Lynass¹, Oleg Sulima² & Oliver Mayer¹

¹GE Global Research Europe, Garching, Germany; ²GE Global Research, Niskayuna, New York, USA

ABSTRACT

Electroluminescence (EL) imaging for photovoltaic applications has been widely discussed over the last few years. This paper presents the results of a thorough evaluation of this technique in regard to defect detection in photovoltaic modules, as well as for quality assessment. The ability of an EL system to detect failures and deficiencies in both crystalline Si and thin-film PV modules (CdTe and CIGS) is thoroughly analyzed, and a comprehensive catalogue of defects is established. For crystalline silicon devices, cell breakages resulting from micro-cracks were shown to pose the main problem and to significantly affect the module performance. A linear correlation between the size of the breakages and the power drop in the module was established. Moreover, mechanical stress and temperature change were identified as the major causes of the proliferation of cracks and breakages. For thin-film modules, EL imaging proved the existence of an impressive reduction in the size of localized shunts under the effect of light-soaking (together with a performance improvement of up to 8%). Aside from that, the system voltage was applied in order to monitor transparent conductive oxide (TCO) corrosion effects and laser-scribing-induced failures, as well as several problems related to the module junction box in respect of its sealing and the quality of its electric connectors.

Introduction

Photovoltaic cells are optimized for absorbing light and converting it into electricity. Because of the reciprocity principle, they can also be stimulated to emit photons, thereby offering a basis for optical characterization techniques. In recent years, a variety of optical tools, which in part had been developed for other applications, have been investigated for quality assessment in the photovoltaic industry. Electroluminescence (EL), photoluminescence (PL), laser-beam-induced current imaging (LBIC) and thermal imaging are examples of the best-known techniques.

“EL has been recently integrated as an investigative procedure for photovoltaic devices.”

An optical technique which has been used for many years [1] in lighting applications, EL has been recently integrated as an investigative procedure for photovoltaic devices. It consists of applying a direct current to the module and measuring the photoemission by means of a camera sensitive to near-infrared. The brightness distribution on the imaged crystalline silicon solar modules correlates with the distribution of the open-circuit voltage V_{oc} , the minority carrier diffusion length and the series resistance, as well as with the quantum efficiency and the ideality factor of the examined cell [2–5]. The work at hand focuses on presenting the measurement set-up for EL imaging and evaluating its capabilities regarding

quality assessment and defect detection in solar cells and modules of different technologies.

EL measurement system

Equipment

For this investigation, a back-illuminated Si-CCD camera from Great Eyes with a high near-infrared (NIR) sensitivity (quantum yield 85% @ 750nm, 40% @ 900nm and 10% @ 1000nm) was used. The system features a resolution of 1024 × 1024 pixels and a pixel size of 13μm × 13μm. The dynamic range of the recorded data amounts to 16 bits. The camera is equipped with a Minolta MD W.Rokkor Objective with a focal length of 35mm and a maximum F-number of f/1.8. The system is mounted on a freely adjustable tripod inside a black tunnel, allowing both close-up measurements of different module sections (with a minimum camera–object distance of 30cm) and overall shots of complete modules. The 5.5m tunnel length is suitable for full-size images of all common panel sizes up to 2m × 2m.

The power supply is ensured by a TDK-Lambda GEN300-11 programmable DC unit with a maximum voltage output of 300V and a maximum current output of 11A. The integrated synchronization module allows control of the EL camera as well as communication with the measurement software. The user–system interaction is based on the LumiSolar Mobile software. In general, the power supply should be chosen in such a way that the maximum applicable voltage and current are at least 120% of the respective

values of open-circuit voltage (V_{oc}) and short-circuit current (I_{sc}) of the module under test.

The system validation was performed, through a qualitative and quantitative comparison of EL measurements of two reference modules, by the system at GE Global and by an electroluminescence set-up at the Fraunhofer ISE research centre in Freiburg.

System parameter optimization

Aperture size and exposure time

Images can only be sharpened to the extent that the quality of the focal lens and of the photo detector allows. A smaller aperture size improves the sharpness of an image and makes it less sensitive to optical aberrations. However, this comes at the cost of a lower light exposure, thus resulting in lower counts, which can only be compensated by a higher exposure time. The consequent risk is that different areas might exhibit, over a period of time, a changing behaviour in photoemissions, due to heating. The linearity of the EL signal was therefore analyzed within different areas of the module and is shown in Fig. 1.

The averages of the pixel grey values were calculated (i) for the whole module – blue diamonds in Fig. 1(b); (ii) for a rectangle including a shunted cell – red inset in Fig. 1(a) and red squares in Fig. 1(b); and (iii) for a small rectangle of 2 pixels × 5 pixels at the bright spot of a shunt – orange rectangle in Fig. 1(a) and orange circles in Fig. 1(b). As can be seen from the linear fits (red lines in Fig. 1(b)), the EL signal increases linearly with the integration time for all three selections

Fab & Facilities

Materials

Cell Processing

Thin Film

PV Modules

Power Generation

Market Watch

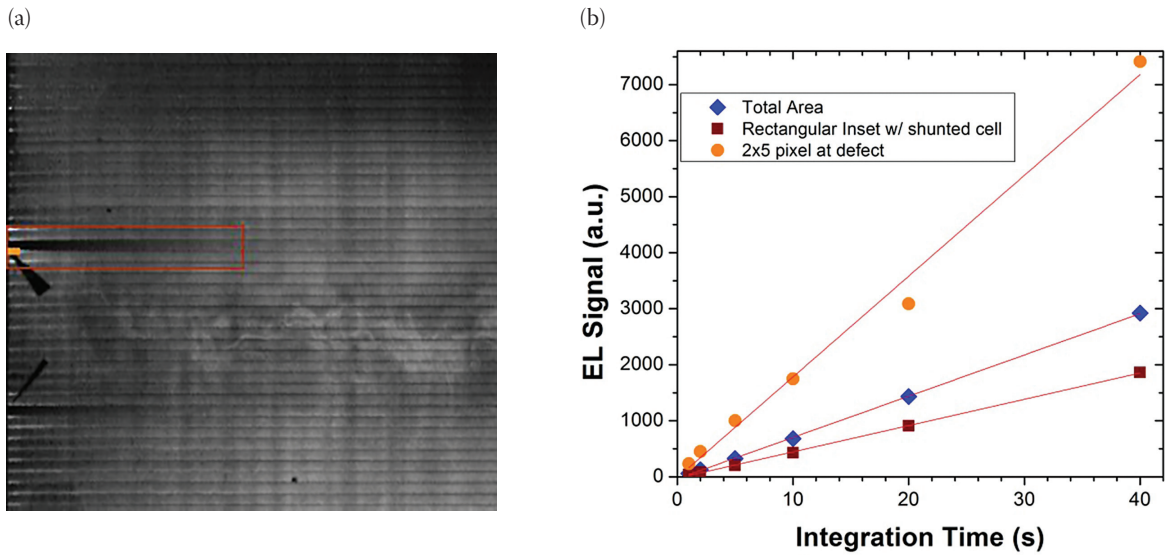


Figure 1. (a) Section of a CdTe module with the analyzed areas indicated. (b) EL signal intensity at different integration times for different areas of the CdTe module.

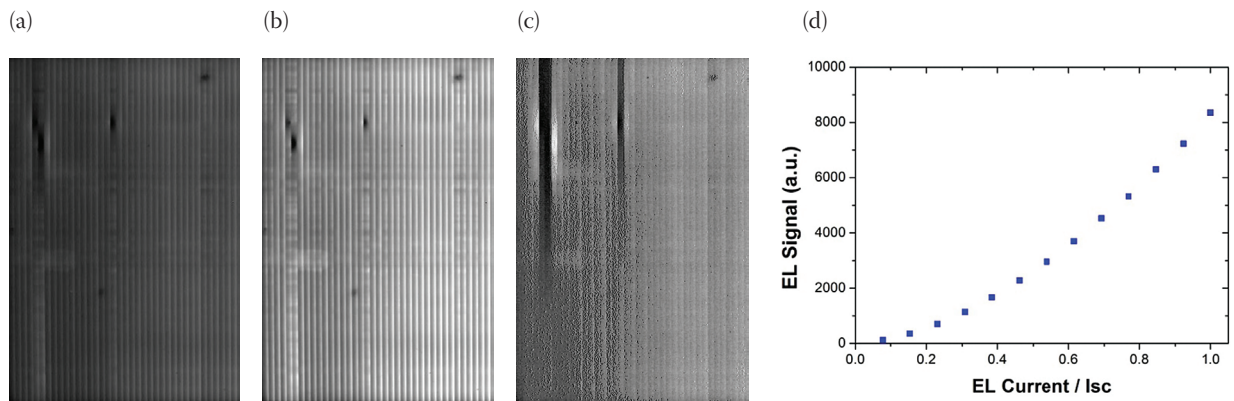


Figure 2. Influence of current on EL signal strength, taken at (a) $0.5 \times I_{sc}$ and 60s; (b) $1.0 \times I_{sc}$ and 60s; and (c) $0.15 \times I_{sc}$ and 60s (brightness up-scaled 15 \times). (d) Mean grey value over different currents.

($R^2 > 0.99$ for all data sets). Hence it is concluded that, with integration times of 40s and currents close to the I_{sc} of the module, non-linearity effects caused by module heating are negligible. In general, an integration time of 10–30s at excitation currents close to I_{sc} was sufficient to achieve a high image quality and a good signal-to-noise ratio.

radiatively. The diffusion process, and thus the current, increases almost instantly when the applied voltage reaches the V_{oc} level. In order to prevent the power supply from damaging the module, it is recommended to operate the excitation power supply in constant current mode. The excitation current should also not

exceed 120% of the device's I_{sc} . Comparing EL images with different currents allows different types of defects to be identified, as shown in Fig. 2. Shunted cells can be easily recognized, as their area of influence (the screening length of a shunt) decreases with a higher current. Images with a very low applied bias can be very useful for

“Comparing EL images with different currents allows different types of defects to be identified.”

Operating voltage and current

The purpose of applying an electric voltage during the EL imaging is to counter the electric field in the depletion zone, thus allowing the charge carriers to diffuse into the p-n junction and to recombine

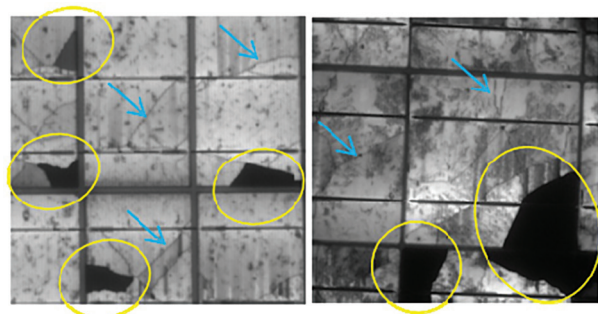


Figure 3. Cracks and breakages in crystalline silicon cells.



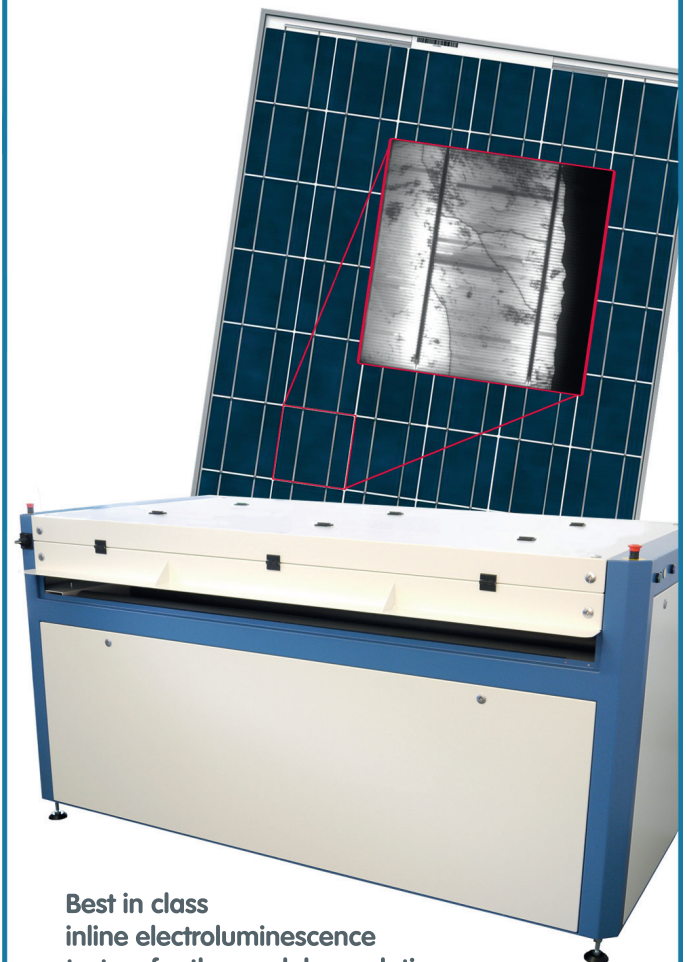
Electroluminescence Inspection Systems from MBJ Solutions Germany

Available models:

- SolarModule EL-inline eco **NEW low budget**
- SolarModule EL-inline 25
- SolarModule EL-inline
- SolarModule EL-inline HS **NEW 200 MWp**
- SolarModule EL-inline HR **NEW 240 MPixel**

New models with higher speed (up to 200MW) and higher resolution (100µm/px or 240 MPixel) for fully automatic lines available.

New low budget eco line versions are offering a good image quality (15 MPixel) together with the best in class machine concept.



**Best in class
inline electroluminescence
testers for the module production.**

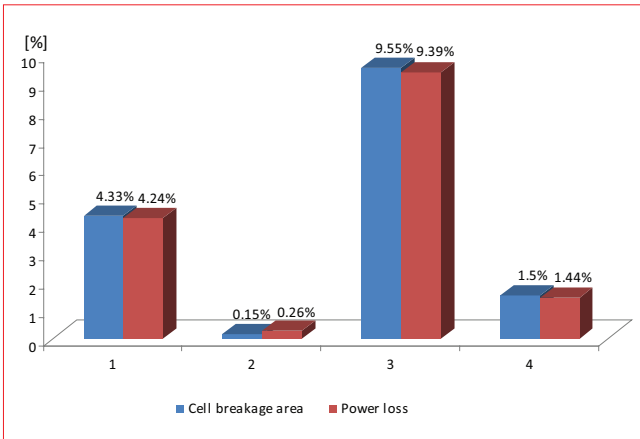


Figure 4. Correlation between cell breakage area and power loss.

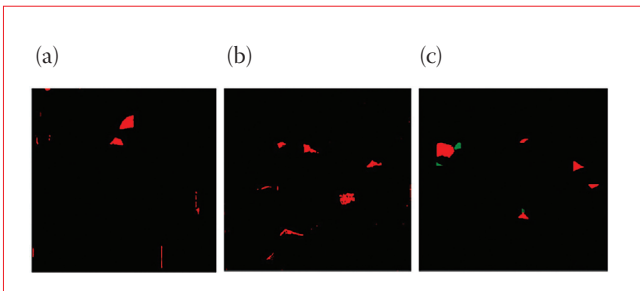


Figure 5. Propagation of cell cracks and breakages in a c-Si module under different stress conditions: (a) mechanical load test; (b) hail test; and (c) thermal cycling.

visualizing the effect of diode shunts, but a lot of the contrast and spatial resolution of the defects is lost. Differential images of the same module at different currents are probably the best for revealing these phenomena.

Defects in crystalline silicon modules

Cracks and breakages

Cracks and breakages in the semiconductor material are responsible for the majority of cases of power loss in crystalline silicon cells. Cracks generally impact only a small line and hence do not severely affect the output power [6]. However, they can also damage the contact fingers, resulting in the development of cell breakages, especially if the crack propagates in a direction perpendicular to the fingers. Fig. 3 shows the typical appearance of cell cracks (blue arrows) and breakages (yellow circles) in crystalline silicon cells. The contact fingers are aligned vertically in these images.

To accurately assess the impact of cell breakages on device performance, the output power of four modules of different sizes was measured in a flash solar simulator. For each module, an EL measurement was taken, and the breakage areas – appearing dark in the EL image (grey values under a certain threshold) – were integrated. A direct correlation between the total breakage area and the power drop was clearly observed. The comparison results are shown in Fig. 4.

In the search for the reasons behind the occurrence and propagation of cell cracks and breakages, several crystalline silicon modules were exposed to different stress conditions and the EL measurements before and after the experiment were compared. All pixels featuring a grey value over a certain threshold and corresponding to the newly formed cracks and breakages are marked in red on the resulting images of the stress tests (Fig. 5).

The application of a mechanical load of approximately 4500Pa to a polycrystalline silicon module (front and rear side) for a duration of two hours induced the occurrence of several new cracks as well as the

MBJ Solutions GmbH

Merkurring 82
22143 Hamburg
Germany

Phone +49 40 606 870 66
Email info@mbj-solutions.com
www.mbj-solutions.com



... just right for your production

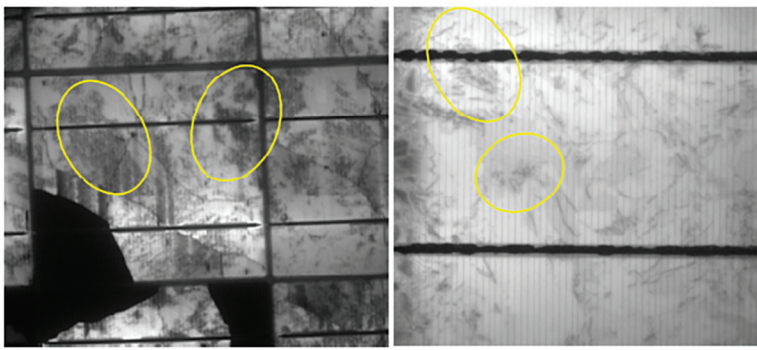


Figure 6. Crystal inhomogeneities in crystalline silicon cells.

development of a number of cell breakages, generally situated between two pre-existing cracks (Fig. 5(a)). Similar effects could be noticed under the influence of punctual, short-term strains, such as the impact of hailstones (simulated using a hail cannon and ice balls according to the endurance-test norm). The corresponding differential image is given in Fig. 5(b). On the other hand, temperature cycling experiments did not show conclusive degradation effects: several modules were exposed to five temperature cycles with a 10-hour period, varying between -40°C and $+85^{\circ}\text{C}$ in the climate chamber. Some cracks and breakages appeared (Fig. 5(c): red areas), but other areas with existing defects regained their activity (Fig. 5(c): green areas). This effect can be explained by the expansion and contraction of the metallic contact fingers through temperature modulation. Depending on their position and depth, contact interruptions due to cell cracks can be restored or extended.

Crystal inhomogeneity

A further imperfection of crystalline silicon cells, which can be easily detected using EL imaging, is crystal inhomogeneity; this appears in the EL image as distributed dark areas with a granular appearance (Fig. 6). These inhomogeneities can have various causes [7], such as process-related fluctuations in dopant concentration or in material thickness, and inherent non-uniformities related to structural defects and to the quality of the material itself.

Defective edge isolation

Short circuits may appear during the edge isolation process. The electric potential difference between the n-doped and p-doped semiconductors of the p-n junction decreases, leading to a weaker detectable EL signal in the measured data. Fig. 7 shows a section of a polycrystalline silicon module with defects in the isolation of the cell edges.

Contact grid interruptions

Flaws in the cell production process can lead to local interruptions/failures of the contact

fingers before or during the contacting operation. Depending on the position and width of the contact gap, the impact of this defect on the module power output can vary greatly. Contact finger interruptions situated on the cell edges pose a particular problem: in the outer fingers of the solar cell, the current is injected by a single busbar, so the finger interruption causes a complete contact outage between the finger gap and the cell edge. In the EL image, these defects are easily detectable in the form of dark areas surrounding the interrupted finger and reaching to the cell edges (blue arrows in Fig. 8).

“Shunts and weak diodes have a very particular EL brightness pattern.”

Defects in thin-film modules

Shunts and weak diodes in light-soaking studies

Shunts and weak diodes are localized between the front and the rear contacts of the solar cell. They result in a lower open-circuit voltage and thus a lower fill factor of the cell. Several mechanisms can be behind the occurrence of shunts and weak diodes, including failures in the deposition

procedure (resulting in a discontinued or a locally too-thin p-type semiconductor layer), faulty laser scribing (inducing p-n junction damage), and the presence of dust particles or metal traces. Shunts and weak diodes have a very particular EL brightness pattern: a localized darkness within a single cell, having a particularly dark centre and a symmetric appearance along the cell. The screening length of shunts and diodes also increases with decreasing excitation current. In the scope of this work, shunts and weak diodes were barely noticeable in crystalline Si modules but are very common in thin-film devices, especially those based on CIGS.

During the investigation of local shunts and weak diodes, it was proved that light-soaking treatment reduces their size considerably and thus their impact on module performance. EL images of a CIGS module after a long-term dark storage are presented in Figs. 9(a) and (b); the corresponding images after the module was treated for 24 hours in the light-soaking station under 1000 W/m^2 are given in Figs. 9(c) and (d). The difference between before and after the light-soaking process is remarkable: a significant reduction in the size of the dark areas surrounding the spots with shunts/weak diodes as well as an increase in operating voltage (+6.3%) and module output power (+8%). Other studies have explained the rise in operating voltage by the light-soaking-induced rise in the charge-carrier density [8,9]. Evidence was found that a reduction in shunts and weak diodes also plays a role here, and further studies are necessary to fully explain the light-soaking enhancement in CIGS solar cells and modules.

Potential-induced degradation (PID)

The corrosion of the transparent conductive oxide (TCO) layer is known to mainly affect modules based on glass substrates when exposed to high negative voltages at high temperatures and humidity levels [10,11]. The corroded front contact interrupts the charge-carrier transport into the junction, and the affected areas appear dark in the EL image.

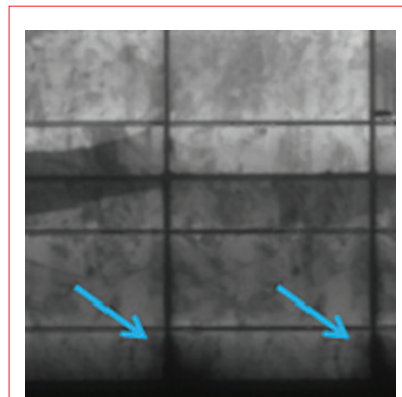


Figure 7. Defective edge isolation.

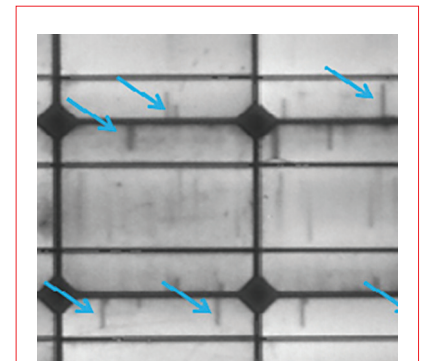


Figure 8. Contact finger interruptions in a monocrystalline silicon cell.

and after the test, as well as at intermediate stages. A dependency between the dark area and the power drop can be seen in Fig. 10. EL allows the identification of the weak points of the module: in this case it is the edge sealing, which allowed moisture penetration, enhancing TCO corrosion. The dark areas are at the edges, whereas no degradation is visible at the junction box. The dark areas do not change in size when different excitation currents are applied and, hence, are not related to shunts and weak diodes but rather to contact layer degradation. It is assumed that TCO corrosion is the major source of degradation observed here.

Laser-scribing failures

Failures can occur during the laser-scribing process for monolithic cell interconnection in thin-film modules. Three scribes are necessary for creating the cell interconnections, as shown in Fig. 11(a). P1 and P3 separate adjacent cells by interrupting the front (P1) and back (P3) contact layers. The purpose of P2 is to provide the connection between the front and back contacts of two neighbouring cells. An interrupted scribing line can result in a shunting bridge over P1 (Fig. 11(b)) or P3 (Fig. 11(c)) in cell A or cell B respectively, and no EL signal is visible close to the bridge.

Fig. 12 shows an example of a module with two different scribing-line bridges (red arrows).

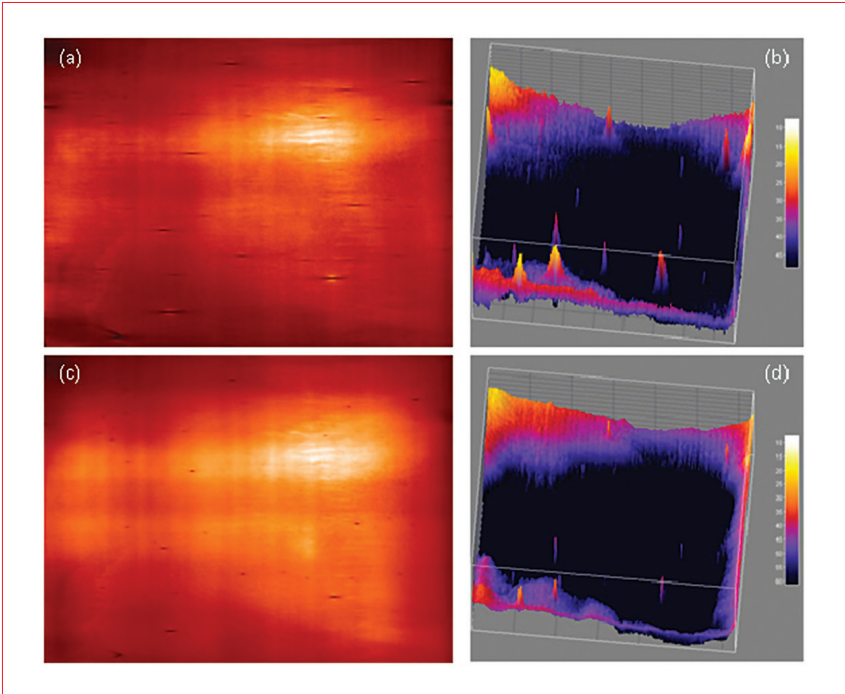


Figure 9. Development of shunts and weak diodes in CIGS-based modules: (a,b) before light-soaking; (c,d) after light-soaking. The colours in images (b) and (d) are inverted for better visualization of defects.

To investigate the correlation between the changes to EL images through PID and the power drop in thin-film panels, a negative potential of 1kV was applied to the shunted contacts of a CdTe-based module while the glass surface was

grounded by gluing to it an aluminium foil that was connected to the ground of the high-voltage source. The module was exposed to 85°C and 85% relative humidity for 250 hours in a climate chamber. Power and EL measurements were taken before

Electroluminescence Imaging For PV-Applications

Module Qualification with coolSamBa HR-830

- High resolution imaging
- Noise-optimized, high sensitivity
- Detailed defect inspection with one shot

Cell Inspection with SamBa Ci

- High throughput, high resolution imaging
- High sensitivity in-line defect inspection
- GigE - fast and robust interface

NEW 16 Megapixel and more per image - Very short working distances



Sensovation's coolSamBa HR-830 and SamBa Ci are ideal cameras for process control in Photovoltaics production, which ensures improved quality and reduced costs of cells and modules. - Please visit our website and request more information.

www.sensovation.com



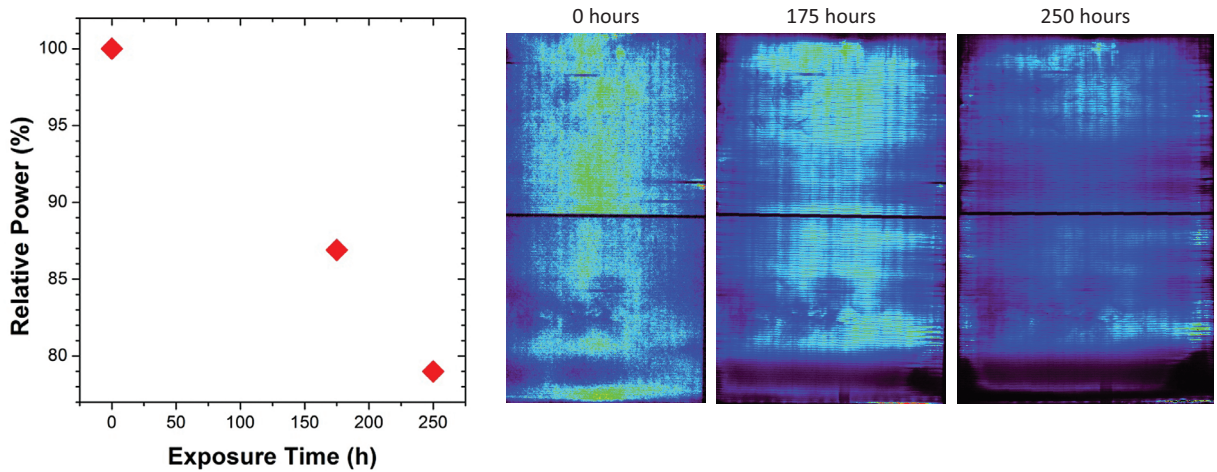


Figure 10. Progression of TCO corrosion in a thin-film CdTe module.

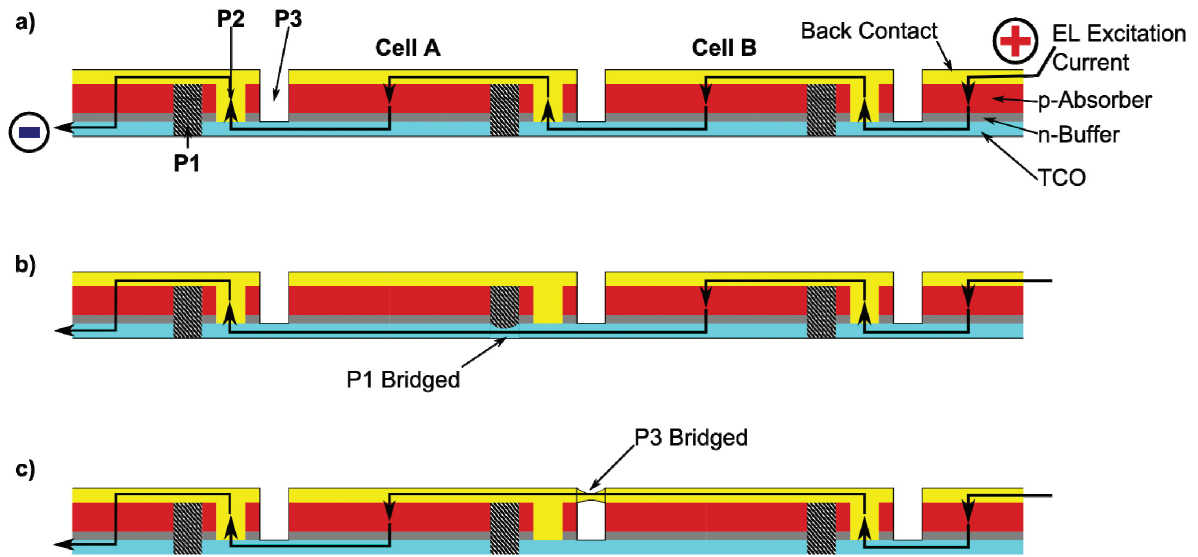


Figure 11. Schematic of the typical monolithic cell interconnection of thin-film modules grown in a superstrate configuration: (a) intact configuration of neighbouring cells; (b) bridged P1 scribe; (c) shunt over the P3 scribe.

“An EL imaging system is capable of accurately detecting numerous failures originating from the cell production process.”

Conclusion

This paper has shown that EL imaging represents a powerful quality assessment tool for both crystalline silicon and thin-film solar modules. When properly adjusted and configured, an EL imaging system is capable of accurately detecting numerous failures originating from the cell production process. Furthermore,

it is a very useful tool for observing and explaining the changes in cell or module performance that are generated by mechanical, electrical or environmental stress tests.

References

- [1] Dupuis, R.D. & Krames, M.R. 2008, “History, development, and applications of high-brightness visible light-emitting diodes”, *J. Lightwave Technol.*, Vol. 26, No. 9, pp. 1154–1171.
- [2] Würfel, P. et al. 2007, “Diffusion lengths of silicon solar cells from luminescence images”, *J. Appl. Phys.*, Vol. 101, p. 123110.
- [3] Fuyuki, T. et al. 2006, “Analytic findings in the photographic characterization of crystalline silicon

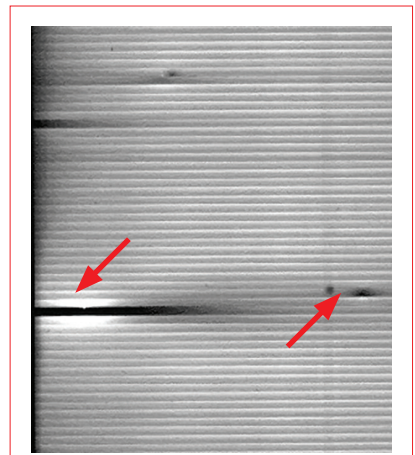


Figure 12. Scribing-line bridges in a CdTe thin-film module (image taken at 650mA and 40s).

- solar cells using electroluminescence”, *Proc. IEEE 4th World Conf. PV Energy Conver.*, Waikoloa, Hawaii, USA.
- [4] Köntges, M. et al. 2009, “Quantitative analysis of PV-modules by electroluminescence images for quality control”, *Proc. 24th EU PVSEC*, Hamburg, Germany.
- [5] Hinken, D. et al. 2007, “Series resistance imaging of solar cells by voltage dependent electroluminescence”, *Appl. Phys. Lett.*, Vol. 91, p. 182104.
- [6] Zimmermann, C.G. 2006, “Utilizing lateral current spreading in multijunction solar cells: An alternative approach to detecting mechanical defects”, *J. Appl. Phys.*, Vol. 100, p. 023714.
- [7] Salinger, J., Benda, V. & Macháček, F.Z. 2008, “Optimal resolution of LBIV/LBIC methods for diagnostics of solar cell homogeneity”, *Proc. 26th Int. Conf. Microelectron.*, Niš, Serbia.
- [8] Igalson, M., Cwil, M. & Edoff, M. 2007, “Metastabilities in the electrical characteristics of CIGS devices: Experimental results vs. theoretical predictions”, *Thin Solid Films*, Vol.

515, pp. 6142–6146.

- [9] Haug, F.-J. et al. 2003, “Light soaking effects in Cu(In,Ga)Se₂ superstrate solar cells”, *Thin Solid Films*, Vol. 431–432, pp. 431–435.
- [10] Carlson, D.E. et al. 2003, “Corrosion effects in thin-film photovoltaic modules”, *Prog. Photovolt.: Res. Appl.*, Vol. 11, pp. 377–386.
- [11] Jansen, K.W. & Delahoy, A.E. 2003, “A laboratory technique for the evaluation of electrochemical transparent conductive oxide delamination from glass substrates”, *Thin Solid Films*, Vol. 423, pp. 153–160.

About the Authors



Amine Mansouri is a researcher within the Solar Lab at GE Global Research Europe in Garching, Germany.



Martin Bucher is a researcher within the Solar Lab at GE Global Research Europe.



Frederick Koch is a Master's student at GE Global Research Europe.

Marcus Zettl leads the Solar Lab at GE Global Research Europe.

Omar Stern is a senior scientist in solar technologies at GE Global Research Europe.

Mark Lynass is head scientist in solar at GE Global Research Europe.

Oleg Sulima is a senior photovoltaic scientist at GE Global Research in Niskayuna, New York, USA.

Oliver Mayer is the principal scientist in solar systems at GE Global Research Europe.

Enquiries

GE Global Research Europe
Freisinger Landstr. 50
85478 Garching
Germany